Cation vacancies in doped zirconolite ($CaZrTi_2O_7$)

J. H. HADLEYJR., F. H. HSU
Department of Physics and Astronomy, Georgia State University, Atlanta, GA 30303, USA

E. R. VANCE, M. COLELLA, K. L. SMITH, G. R. LUMPKIN, M. L. CARTER, B. D. BEGG
Materials and Engineering Science, ANSTO, Menai, NSW 2234, Australia

Published online: 16 September 2005

Zirconolite ($CaZrTi_2O_7$) is a key phase in synroc-type titanate ceramics [1, 2] for immobilising high-level nuclear waste, partitioned actinides, and surplus weapons plutonium. The structure of undoped zirconolite is an anion-deficient derivative fluorite structure having the C2/c space group. Zirconolite solid-solutions of the type $CaZr_xTi_{3-x}O_7$, where x ranges from 0.7 to 1.3, crystallise as the 2M polytype. Numerous studies [3, 4] of the incorporation of lanthanide and actinide elements in zirconolite have shown that other polytypes such as 3T, 3O, and 4M occur with increasing levels of substitution on the Ca- and Zr-sites. The appearance of these polytypes is dependent upon the type of substitution and the temperature and oxygen fugacity during fabrication.

Only recently has it been realised that several percent of cation vacancies may be present in rare-earth doped zirconolites which were mainly of the 3T or 4M polytypes [5] through diffraction studies. Careful stoichiometric studies via electron microscopy and positron annihilation lifetime spectroscopy (PALS) [6] indicated significant vacancy contents in oxidised Ce-doped 2M zirconolites. PALS is especially sensitive to cation vacancies because of the Coulombic attraction of positrons to these negative regions which can lead to positron "trapping" at these sites. Because of the low electron density at such vacant sites, "trapping" will be observed as an increased annihilation lifetime of these positrons.

The major PALS spectral component in zirconolite is characterised by the shortest resolved positron lifetime, τ_1, and increases in τ_1 for this component, which includes a contribution due to positron trapping, of ~20% were observed in the oxidised Ce-doped zirconolite samples containing ~0.02 or 0.04 f.u. of cation vacancies, deduced from analytical electron microscopy (depending on whether the vacancies derived from Ti or Ca sites, respectively). PALS in a range of $Sr_{(1-3x/2)}La_xTiO_3$ perovskites showed that τ_1 increased rapidly with vacancy content, and the increase saturated at a value of ~20% when more than ~0.05 f.u. of Sr vacancies were present [6]. The magnitudes of these lifetime increases give an approximate metric for the vacancy contents of these kinds of titanate phases, except for the saturation effects at vacancy contents greater than ~0.05 f.u.

The maintenance of electroneutrality in ionic solids is of fundamental interest and aliovalent ionic substitutions can be accommodated by a variety of charge compensating species. These include cation and anion vacancies, interstitals, and combinations of these. When the substitution is extensive, these defects significantly impact on the chemical composition of the phase, and this in turn influences the physical properties. In the present case of candidate waste forms for immobilisation of radioactive waste, the design of the phase requires knowledge of the charge compensating species and also the response to self-irradiation from especially alpha-emitting actinides can depend on the presence or otherwise of pre-existing vacancies [7].

We have attempted in the first instance to create Ca site vacancies in 2M zirconolite via two trivalent Gd ions substituting for three Ca ions using stoichiometric measurements from electron microscopy and PALS to detect the vacancies. For comparison, charge-compensated (Gd,Al)-doped 2M-zirconolites, and a near single-phase 4M zirconolite were also studied, together with two Nd-bearing zirconolite compositions which were argued to contain Ca vacancies by Coelho [5].

Zirconolite samples were prepared by mixing Ti and Zr alkoxides with aqueous metal nitrate solutions, drying, calcining at 750 °C, and wet ball-milling; then pellets were cold-pressed and sintered for several days at 1400 °C in an air atmosphere.

Scanning electron microscopy (SEM) on polished surfaces of samples was carried out on a JEOL 6400 machine run at 15 kV and fitted with a Tracor Northern TN5502 energy-dispersive spectrometer (EDS) which utilised a comprehensive range of standards for quantitative work. The stoichiometric accuracy is around ±0.02 f.u. [8] and the averages of around four separate sample regions were taken. A JEOL 2000FXII transmission electron microscope was run at 200 kV and the EDS data were obtained from a Link ISIS Si(Li) solid state detector and multichannel analysis system. Again the stoichiometric accuracy is in the order of ±0.02 f.u. [9]. X-ray diffraction (XRD) was performed with a Siemens D500 instrument employing Co Kα radiation.

For PALS a conventional fast-fast lifetime spectrometer employing plastic scintillators was used, with a

0022-2461
DOI: 10.1007/s10853-005-4559-y

^{22}Na source sandwiched between two pieces of sample material. A time resolution of 0.320 ns was measured for a ^{60}Co "prompt" at FWHM under actual experimental conditions. Whereas the "prompt width" is a measure of the time resolution of the spectrometer, it does not represent the minimum lifetime that can be measured. The sample temperature was held at 21 °C using a computer-controlled room HVAC system. A commercially available computer program, POSITRONFIT-EXTENDED, is used to analyse the data. This program determines background and also deconvolutes to remove most of the "prompt curve" (instrumental broadening) before fitting the data (counts versus time) to obtain the lifetime parameters (lifetimes and their corresponding intensities) of up to three spectral components (exponential decays). In the present work, the results show no evidence for the presence of bound positron states such as positronium (a positron–electron "atom") or positrons bound to negative ions. Without significant bound-state formation, most of the positrons decay directly with electrons with a characteristic decay lifetime τ_1 of about 0.2 ns. A small fraction, normally less than 10%, decay within the ^{22}NaCl source itself, or its encapsulation, with a lifetime τ_2 which is typically between 0.4 and 0.5 ns.

In some cases the positron may be briefly "trapped" within an attractive (negative) region within the solid (without forming a more stable bound state) and decay with a lifetime slightly longer than τ_1. The lifetimes of these trapped positrons are not sufficiently longer than that of those decaying directly for a distinct trapped-positron lifetime to be observed. Instead, the decay spectrum is broadened and a composite lifetime τ_1 is measured that is slightly larger than that for direct annihilation without trapping. In the present experiments the maximum increase in τ_1 produced by trapping is about 20%.

Zirconolite samples of $Ca_{(1-3x/2)}Gd_xTi_2O_7$ stoichiometry with $x = 0.02$, 0.1 and 0.2, nominally containing $x/2$ f.u. of Ca vacancies, were first studied. In terms of energy cost it would be expected that the cation site with the lowest charge (Ca) would be favored for vacancy formation.

Electron microscopy and XRD showed that the $x = 0.02$ and $x = 0.1$ samples were basically single phase 2M zirconolite, with a few percent of rutile and $ZrTiO_4$ being present in the latter. The sample with $x = 0.2$ consisted mainly of zirconolite, but there was minor $ZrTiO_4$ and rutile also, in amounts somewhat larger than those in the $x = 0.1$ sample. Table I shows the measured stoichiometries of the zirconolite phase in each of these materials. The (Ca + Gd) content in each zirconolite added to 0.97–0.99 in each case, implying that no more than ~0.03 f.u. of Ca vacancies can be incorporated in the zirconolite structure (neglecting for the moment the experimental error of ~0.02 f.u.-see above) and therefore suggest that the target stoichiometry only applies at small x values, in the range of $x <$ approximately 0.02, if it applies at all. While the (Zr + Ti) added to 3.02 for the $x = 0.02$ sample, it added to 2.97 and 2.95 for the $x = 0.1$ and 0.2 samples, respectively, indicative of Zr/Ti vacancies, although the numbers again border on the experimental errors. The absence of a violet color (due to a broad absorption band centred near 20000 cm^{-1} [10]) suggested that charge compensation through significant amounts of Ti^{3+} were not present in these air-fired samples.

Charge compensation in the $x = 0.1$ and 0.2 samples appears from the measured stoichiometries to result from partial substitution of Gd in the Zr site, to counterbalance any excess charge from Gd in the Ca site that is not compensated by a small number of Ca vacancies. Indeed it is possible that Ti/Zr vacancies in the zirconolite could compensate the entire excess charge from Gd on the Ca site in these samples. For example 0.05 f.u. of Ti/Zr vacancies could charge compensate for the excess charge occasioned by 0.2 f.u. of Gd on the Ca site and these numbers would be in agreement within experimental error of the measured stoichiometries in the $x = 0.2$ sample. If the vacancies were on the Ti sites alone, the experimental appearance of rutile would be expected and in conjunction with the Zr content (0.95 f.u.) of the zirconolite phase being <1.00 f.u., the appearance of the $ZrTiO_4$ phase is also explained.

The PALS results in terms of intensities and lifetimes of spectral components are shown in Table II. Each spectrum was fitted to two lifetimes. The data showed a ~20% increase in the majority short lifetime τ_1 relative to the undoped sample in all the doped samples, and the increase is attributed to at least 0.02 f.u. of cation vacancies in the zirconolite lattice in each case.

As a comparison for the samples above, it was of interest to prepare charge-compensated samples in which the excess charges on the Gd ions substituted in the Ca site were compensated by equal numbers of Al ions substituted in the Ti sites. Table III gives these results. Although little change occurred even when half the Ca

TABLE I Measured stoichiometries of nominal $Ca_{(1-3x/2)}Gd_xZrTi_2O_7$ samples

x	Ca	Gd	Zr	Ti
0.02	0.95	0.02	0.99	2.03
0.1	0.88	0.10	0.98	2.00
0.2	0.78	0.21	0.95	2.00

TABLE II PALS parameters for Gd-doped zirconolites of nominal $Ca_{(1-3x/2)}Gd_xZrTi_2O_7$ stoichiometry

Composition	τ_1 (ns)	I_1 (%)	τ_2 (ns)	I_2 (%)
$CaZrTi_2O_7$	0.227	92.3	0.484	7.7
$Ca_{0.97}Gd_{0.02}ZrTi_2O_7$	0.277	97.8	0.648	2.2
$Ca_{0.85}Gd_{0.10}ZrTi_2O_7$	0.280	98.4	0.737	1.6
$Ca_{0.70}Gd_{0.20}ZrTi_2O_7$	0.271	97.1	0.626	2.9

TABLE III PALS parameters for compensated (Gd,Al)-doped zirconolites

Composition	τ_1 (ns)	I_1 (%)	τ_2 (ns)	I_2 (%)
$CaZrTi_2O_7$	0.227	92.3	0.484	7.7
$Ca_{0.5}Gd_{0.5}ZrTi_{1.5}Al_{0.5}O_7$	0.231	92.3	0.486	7.7
$Ca_{0.25}Gd_{0.75}ZrTi_{1.25}Al_{0.75}O_7$	0.280	98.5	0.805	1.4

TABLE IV Positron annihilation parameters for Nd- and (Gd,Hf)-doped zirconolites

Composition	τ_1 (ns)	I_1 (%)	τ_2 (ns)	I_2 (%)
$CaZrTi_2O_7$	0.210	83.6	0.416	16.4
$Ca_{0.765}Nd_{0.513}Zr_{0.770}Ti_{1.988}O_7$	0.271	92.0	0.478	8.0
$Ca_{0.715}Nd_{0.218}Zr_{0.979}Ti_{1.988}O_7$	0.261	88.0	0.439	12.0
$Ca_{0.5}GdHf_{0.5}Ti_2O_7$	0.275	95.1	0.544	4.7

Note. The value of τ_1 in Table IV for pure zirconolite differs somewhat from that given in Tables II and III. This is primarily due to changes in spectrometer resolution (Table IV data were measured about a year after the Tables II and III data). This does not affect our experimental conclusions since the data presented for the doped samples were collected, in each case, sequentially with that for pure zirconolite.

is replaced by Gd, a 20% increase in τ_1 was produced by 75% replacement of the Ca. In addition, a nominally single-phase 4M composition of $Ca_{0.5}GdHf_{0.5}Ti_2O_7$ [11] also showed a PALS short lifetime τ_1 of 0.275 ns (see Table IV), ~20% longer than the value for undoped zirconolite (see above and Table II). Given that quite heavy doping in the $Ca_{0.5}Gd_{0.5}ZrTi_{1.5}Al_{0.5}O_7$ sample (see Table III) produced little if any increase in τ_1 relative to pure zirconolite, it would seem that these other samples in which τ_1 is up to 20% larger than the pure zirconolite value contain modest amounts (~0.05 f.u.) of cation vacancies.

Two further samples were made, following work by Coelho [5] in which the presence of cation vacancies in a majority zirconolite phase was deduced from Rietveld X-ray structural analysis. The first sample nominally consisted of the 4M polytype, of composition $Ca_{0.715}Nd_{0.513}Zr_{0.770}Ti_{1.988}O_7$, corresponding to a (theoretical) cation vacancy content of 0.014 f.u. (Ca vacancies) or 0.007 f.u. of Ti/Zr vacancies by assuming 7 oxygen ions per formula unit and adding up the ionic charges on the cations (taken as +2, +3 and +4 for Ca, Nd and Ti/Zr, respectively).

From SEM our sample consisted of a major $Ca_{0.65}Nd_{0.55}Zr_{0.75}Ti_2O_7$ polytype of zirconolite, plus a minor $Ca_{0.70}Nd_{0.29}Zr_{0.94}Ti_{2.00}O_7$ zirconolite phase (see Fig. 1). The implied cation vacancy contents of these phases were 0.05 and 0.07 f.u., respectively for Ca vacancies and half these values for Ti/Zr vacancies, using the methodology above to calculate these quantities. Although XRD indicated that the sample mainly consisted of the 4M polytype, as indicated by a reflection at a *d* spacing of ~1.1 nm [5], TEM (on a small sample) indicated mainly the 3T polytype. Further work is required to resolve this discrepancy. The PALS lifetime τ_1 was 0.271 ns (see Table IV), ~20% higher than that for undoped zirconolite [6] and therefore indicative of >0.02 f.u. of cation vacancies (see above).

The second sample had been shown [5] to exist mainly as the 3T polytype of zirconolite, and had a nominal formula of $Ca_{0.765}Nd_{0.218}Zr_{0.979}Ti_{1.975}O_7$, corresponding to a (theoretical) cation vacancy content of 0.063 f.u. (Ca) or 0.032 f.u. (Ti/Zr). The scanning electron microscope analysis of the sample (Fig. 2) fabricated in the present work showed the major zirconolite phase to be of composition $Ca_{0.71}Nd_{0.25}Zr_{0.95}Ti_{2.00}O_7$ (implied cation vacancy content 0.09 f.u), plus minor $ZrTiO_4$ and rutile. XRD did not indicate the presence of any 4M material. The measured PALS lifetime τ_1 was 0.261 ns (see Table IV), ~15% longer than for pure 2M zirconolite [6], and indicative of 0.01–0.02 f.u. of cation vacancies.

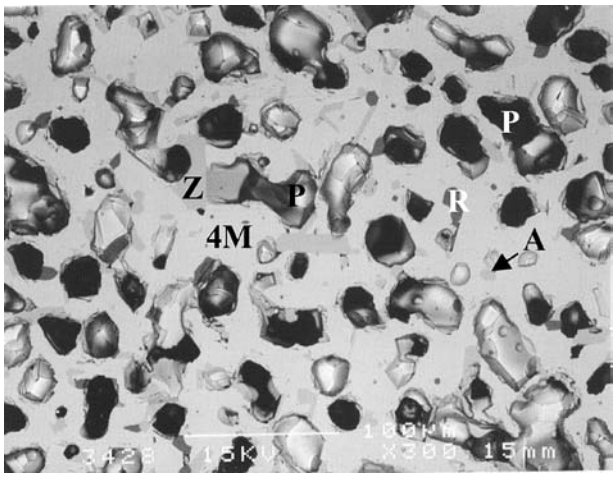

Figure 1 SEM backscattered electron micrograph of $Ca_{0.715}Nd_{0.513}Zr_{0.770}Ti_{1.988}O_7$. 4M = $Ca_{0.65}Nd_{0.55}Zr_{0.75}Ti_2O_7$ (majority phase), Z = $Ca_{0.70}Nd_{0.29}Zr_{0.94}Ti_{2.00}O_7$ (minor zirconolite phase), R = rutile, A = $ZrTiO_4$ and P = pore. Bar = 100 μm. Both the minor zirconolite phase and the $ZrTiO_4$ appear a similar grey color.

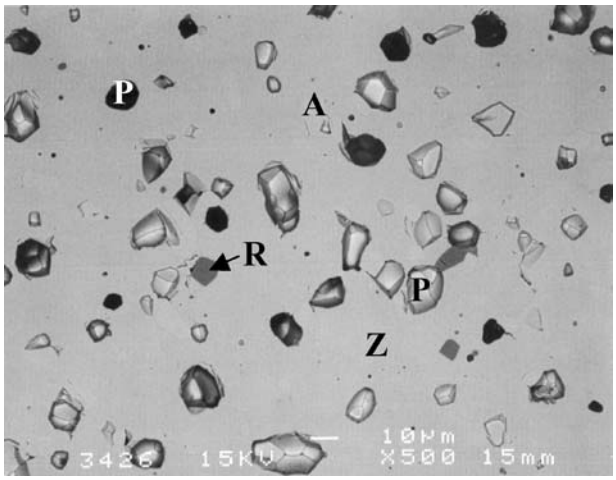

Figure 2 Backscattered electron micrograph of Nd-doped sample of $Ca_{0.765}Nd_{0.218}Zr_{0.979}Ti_{1.975}O_7$ stoichiometry. Z = $Ca_{0.71}Nd_{0.25}Zr_{0.95}Ti_{2.00}O_7$ (majority zirconolite phase), R = rutile, A = $ZrTiO_4$ and P = pore. Bar = 10 μm. Both the zirconolite and the $ZrTiO_4$ appear a similar grey color.

We conclude that cation vacancies may be present at levels of up to 0.05 formula units in zirconolite, depending on the starting stoichiometries, when the materials are prepared by sintering at 1400–1500 °C. The present results offer general but not definitive confirmation of Coelho's conclusions [5] that vacancies are possible in zirconolites doped with rare earths, and it would seem that further careful crystallographic studies using Rietveld analysis of a range of doped zirconolites are necessary to understand the structures and site occupancies in detail.

Acknowledgements

We wish to thank H. Li for assistance with the scanning electron microscopy.

References

1. A. E. RINGWOOD, S. E. KESSON, N. G. WARE, W. HIBBERSON and A. MAJOR, *Nature* **278** (1979) 219.
2. B. B. EBBINGHAUS, R. A. VAN KONYNENBURG, F. J. RYERSON, E. R. VANCE, M. W. A. STEWART, A. JOSTSONS, J. S. ALLENDER, T. RANKIN and J. CONGDON, Waste Management '98 (CD-ROM; sess65/65-04), Tucson, AZ, USA (1998).
3. K. L. SMITH and G. R. LUMPKIN, in "Defects and Processes in the Solid State: Geoscience Applications, the McLaren Volume," edited by J. N. Boland and J. D. Fitz Gerald (Elsevier, Amsterdam, 1993) p. 401.
4. E. R. VANCE, G. R. LUMPKIN, M. L. CARTER, C. J. BALL and B. D. BEGG, *J. Am. Ceram. Soc.* **85** (2002) 1853.
5. A. A. COELHO, R. W. CHEARY and K. L. SMITH, *J. Solid State Chem.* **129** (1997) 346.
6. J. H. HADLEY JR., F. H. HSU, YONG HU, E. R. VANCE and B. D. BEGG, *J. Am. Ceram. Soc.* **82** (1999) 203.
7. K. L. SMITH, M. G. BLACKFORD, M. COLELLA, C. J. HOWARD, Z. ZHANG, G. R. LUMPKIN and N. J. ZALUZEC, "The Effect of Structure and Pre-existing Vacancies on the Radiation Resistance of Perovskite," (Spring Meeting of Materials Research Society, San Francisco, CA, USA, 2004).
8. E. R. VANCE, R. A. DAY, Z. ZHANG, B. D. BEGG, C. J. BALL and M. G. BLACKFORD, *J. Solid State Chem.* **124** (1996) 77.
9. G. R. LUMPKIN, K. L. SMITH, M. G. BLACKFORD, R. GIERE and C. T. WILLIAMS, *Micron* **25** (1994) 581.
10. D. S. MCCLURE, *J. Chem. Phys.* **36** (1962) 2757.
11. D. S. PERERA, R. A. DAY, M. W. A. STEWART, G. R. LUMPKIN and E. R. VANCE, in "Environmental Issues and Waste Management Technologies in the Ceramic and Nuclear Industries VI," edited by D. R. Spearing, G. L. Smith and R. L. Putnam (American Ceramic Society, Westerville, OH, USA, 2001) p. 159.

Received 15 April 2004
and accepted 3 February 2005